

Seismic anisotropy in ocean basins: Resistive drag of the sublithospheric mantle?

Andréa Tommasi, Alain Vauchez, and Raymond Russo

Laboratoire de Tectonophysique, ISTEEM, CNRS/USTL, Montpellier, France

Abstract. We use finite-element models to evaluate the effect of asthenospheric strain associated with the motion of an oceanic plate over a presumed stationary mantle on shear wave splitting observations. Modeled velocity profiles display a clear strain localization within a horizontal shear zone several tens of kilometers wide developed between an almost rigid mechanical lithosphere and a mildly deformed upper mantle. For young oceanic lithosphere, cooling results in migration of the maximum shear strain rate towards deeper levels and progressive widening of the shear zone. Shear strain accumulates with plate displacement. The deformed layer thickness depends on plate age and velocity. Seismic anisotropy depends on the preferred orientations of olivine developed, and thus on the strain field. For a ray propagating vertically (e.g., SKS) the fast wave will be polarized parallel to the flow direction, i.e., the APM. The delay time will depend on the thickness of the sheared layer and on its intrinsic anisotropy. It will therefore increase away from the ridge at a progressively decreasing rate and depend on the absolute plate velocity. The estimated anisotropies agree with seismic anisotropy measurements in old domains of ocean basins, suggesting that, away from mid-ocean ridges, this simple model may provide a first approximation of the mechanism responsible for the observed seismic anisotropy.

Introduction

The relationship between upper mantle flow and plate tectonic processes remains a fundamental problem of geodynamics. Shear wave splitting can be used to probe the seismic anisotropy of the upper mantle [e.g., *Silver and Chan, 1988; Vinnik et al., 1989*]. This anisotropy is related to lattice preferred orientation of elastically anisotropic minerals and thus to the deformation that generates this fabric [*Nicolas and Christensen, 1987*]. The main along-path contribution to splitting comes from the upper mantle [*Mainprice and Silver, 1993; Meade et al., 1995*]. However, is the anisotropy related to a lithospheric mantle fabric due to plate-boundary processes [e.g., *Silver and Chan, 1991*], or to an asthenospheric fabric developed in the upper mantle by resistive drag beneath a moving rigid plate [e.g., *Vinnik et al., 1992*]?

We use finite-element models to evaluate the contribution of asthenospheric strain associated with the motion of a plate over a presumed stationary mantle (i.e., the plate motion relative to assumed fixed hotspots - APM) to shear wave splitting observations. *Froidevaux and Schubert [1975]* and *Schubert et al. [1976]* showed that this deformation is accommodated in a relatively narrow shear zone whose location and thickness depend on the rheological law describing the behavior of the upper

mantle and on the thermal state of the plate (i.e., the age of the plate for oceanic plates). Our models aim to investigate the resulting finite strain field and the effects of plate cooling. We model the deformation beneath an oceanic plate because it should have a simpler geometry and history than a continental plate. Moreover, away from oceanic ridges or hotspots, a velocity gradient between the plate and the deep mantle probably dominates the development of a structured fabric in the uppermost mantle, allowing us to compare our model results with seismic anisotropy measurements in ocean basins.

Model

Our vertical plane-strain model simulates the deformation induced by a difference in velocity between an oceanic plate and the underlying mantle. The plate and underlying upper mantle are simulated by a homogeneous material able to deform by dislocation creep following a dry dunite constitutive relation (Table 1). The least constrained rheological parameter is the activation volume [see *Karato and Wu, 1993*]. Unfortunately, this parameter has a significant effect on the effective viscosity and, thus, on the velocity profiles [*Froidevaux and Schubert, 1975*]. In most models, we use low activation volumes that result in maximum estimates of the deformed layer thickness.

The upper boundary of the model is submitted to a constant velocity (1.5, 3, or 6 cm/y) simulating the plate motion, whereas the lower boundary (at 400 km depth) is fixed. Temperatures of 273K and 1775 K are fixed at the upper and lower boundaries, respectively, and a null heat flux is prescribed at the lateral boundaries. The initial temperature field consists of a 2 My old oceanic plate geotherm calculated using an instantaneous cooling half-space model and an adiabatic gradient in the sublithospheric mantle. Convective heat transfer in the sublithospheric mantle is simulated through an enhanced thermal conductivity (Table 1).

Finite strain

Model velocity profiles (Fig. 1) confirm the results of *Froidevaux and Schubert [1975]* and *Schubert et al. [1976]*. There is a clear strain localization with development of a shear

Table 1. Model Parameters

volumic mass, ρ [kg.m ⁻³]	3350.
heat capacity, C [W.kg ⁻¹ .K ⁻¹]	1100.
heat conductivity - lithosphere, k_L [W.m ⁻¹ .K ⁻¹]	3.5
heat conductivity - asthenosphere, k_A [W.m ⁻¹ .K ⁻¹]	4.67
material constant, A [Pa ⁻ⁿ .s ⁻¹] ^a	2.42e-16
activation energy, E^* [kJ.mol ⁻¹] ^a	540.
activation volume, V^* [m ³ .mol ⁻¹] ^a	1.7e-5
stress exponent ^a	3.5

^a dry dunite dislocation creep flow law [*Karato and Wu, 1993*]

Copyright 1996 by the American Geophysical Union.

Paper number 96GL02891.
0094-8534/96/96GL-02891\$05.00

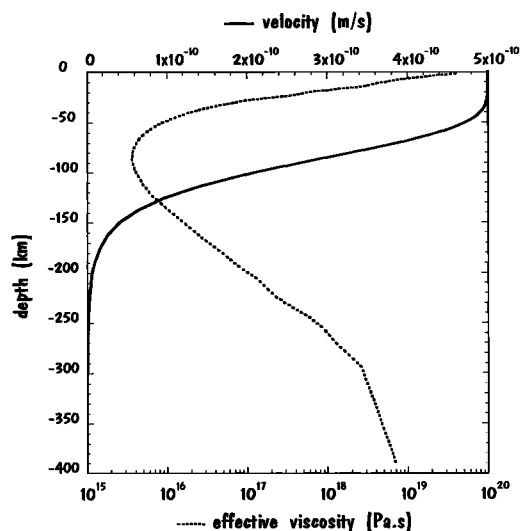


Figure 1. Effective viscosity (dashed line) and velocity (full line) profiles for a 62 My-old slow plate ($v = 1.5$ cm/y).

zone ca. 100 km wide between an almost rigid mechanical lithosphere and mildly deformed upper mantle. This shear zone is associated with a low-viscosity layer induced by the double dependence of the effective viscosity on pressure and temperature. The shear strain rate profile (Fig. 2) is asymmetric across the shear zone: whereas the upper boundary is characterized by a strong shear strain rate gradient, the lower limit displays a gradual decrease of shear strain rate.

Shear strain (γ) accumulates progressively with plate displacement. For young oceanic lithosphere, the upper part of the deformed layer freezes as the plate cools (Fig. 2). Cooling induces a progressive deepening and widening of the low-viscosity layer, and a migration of the maximum shear strain rate towards deeper levels. Seismic anisotropy in oceanic basins is therefore generated in two distinct layers: a frozen lithospheric layer and an asthenospheric layer that records current absolute plate motion.

The total deformed layer thickness depends on the plate age and velocity: for a similar displacement, faster plates accumulate larger shear strains over a thinner layer (Fig. 3). The thickness of this layer (Fig. 4) increases rapidly with plate age for young plates, due to plate cooling and related deepening of the shear zone. This increase slows progressively, and for plates of similar ages the deformed layer thickness depends on plate velocity.

Fabric development and seismic anisotropy

The seismic anisotropy associated with the modeled finite strain field depends on the olivine lattice preferred orientation induced by this deformation [Nicolas and Christensen, 1987]. For a vertically propagating shear wave (e.g., SKS) the fast wave will be polarized parallel to the flow direction [Mainprice and Silver, 1993], i.e., to the APM. The delay time will depend on the sheared layer thickness and on the intensity of crystallographic fabrics, which is controlled by the strain intensity. However, this relationship is still poorly known. Numerical simulation of fabric development in simple shear [Mainprice and Silver, 1993] shows, for $\gamma = 2$, preferred orientations similar to those observed in natural peridotites. Strong fabrics at $\gamma = 1.5$ has also been reported for dunites experimentally deformed in a simple shear

regime at 1573 K [Zhang and Karato, 1995]. Thus, at asthenospheric temperatures, strong preferred orientations may develop at low shear strains.

Since a quantitative relationship between strain and fabric intensity is still lacking, we assume, as a first approximation, that the entire layer displaying $\gamma \geq 1$ displays a homogeneous anisotropy. In this case, delay time depends only on the deformed layer thickness and on its intrinsic anisotropy. It will therefore

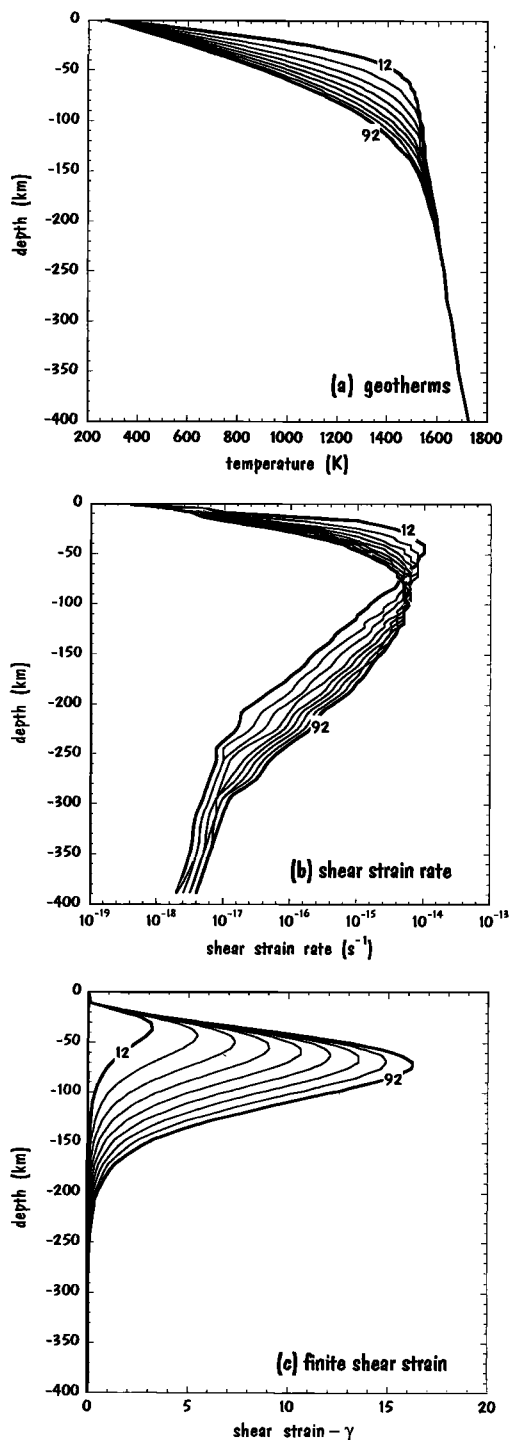


Figure 2. Geotherms (a), shear strain rate (b), and finite shear strain profiles (c) for a slow plate ($v = 1.5$ cm/y) at time intervals of 10 My.

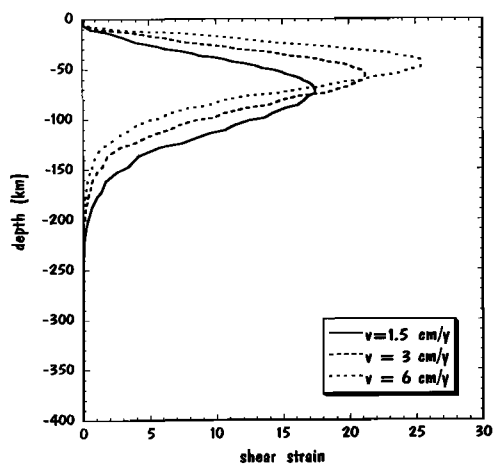


Figure 3. Finite shear strain profiles after 1580 km of displacement for plates displaying different velocities.

increase away from the ridge at a progressively decreasing rate and tend to a maximum value that depends on the plate velocity. For a 180 My-old plate (i.e., the oldest actual oceanic plates), the thickness of the layer displaying $\gamma \geq 1$ varies from 180 km for very slow plates to 250 km for fast plates (Fig. 4). These values are reduced by 20–25 km or 35–45 km if $\gamma \geq 2$ or 3 is used.

To calculate the delay times induced by this layer, the intrinsic anisotropy of a deformed asthenospheric sample must be known. We computed shear wave anisotropy for 5 samples from the Oman ophiolite considered as representative of a "normal" asthenosphere. These samples display no low-temperature deformation and come from deep (3 to 6 km beneath the Moho) and undisturbed (far from asthenospheric diapirs) sections of the ophiolite. For an average sample of composition 70% olivine and 30% pyroxene, the fast wave polarization plane parallels the inferred flow direction and anisotropy is 4.25% in a direction normal to the flow plane. If we apply this anisotropy to the layer displaying $\gamma \geq 1$ in the models, a 180 My-old plate moving at 1.5 cm/y yields delay times for SKS waves up to 1.8 s. Higher plate velocities result in thicker deformed layers and greater delay times (2.1 s for a 180 My-old plate moving at 6 cm/y).

These values are maximum estimates because:

1) Low activation volumes are used in the models. If a higher activation volume ($V^* = 25 \text{ cm}^3/\text{mol}$ [Karato and Wu, 1993]) is used, the thickness of the layer displaying $\gamma \geq 1$ will be reduced by 20–30 km (Fig. 4) and delay times will be 0.17–0.26 s less.

2) Cut-off shear strain values used ($\gamma = 1$) are also low. If $\gamma = 2$ is used, the corresponding delay times will be reduced by ~ 0.2 s.

3) Partial melting is not taken into account in these models. Even small amounts of melt in the asthenosphere may induce a strong strain localization, leading to a thinner sheared layer [Hirth and Kohlstedt, 1995]. Melt may also cause a weakening of petrofabric intensity associated with activation of melt-enhanced diffusion creep or grain boundary sliding.

Comparison with seismic anisotropy data from ocean basins

Keeping in mind that they represent maximum estimates, we may compare our results with splitting measurements in ocean basins. However, most of the available data comes from volcanic island stations in the Pacific: it samples the upper mantle of a

plate that exhibits a marked change in its APM (Hawaii-Emperor chain bend), and that has been partially modified by hotspots.

Our models suggest that old plates (~ 100 My) should be anisotropic down to ca. 200 km. This result is consistent with the depth distribution of surface waves azimuthal anisotropy in the Pacific Ocean [e.g., Montagner and Tanimoto, 1991].

Fast polarization directions in the southern Pacific from SKS splitting [R. Russo and E. Okal, *Geophys. J. Int.*, submitted, 1996; C. Wolfe and P. Silver, *J. Geophys. Res.*, submitted, 1996] are exactly (TPT, Tuamotu Islands) or approximately (RAR, Cook Islands; AFI, Samoa; TBI, Austral Island) parallel to the APM direction. Delay times range from 1 to 1.3 s, except at PPT (Papeete, Tahiti) which is isotropic. These results are consistent with splitting of PS [Su and Park, 1994] and ScS phases [Farra and Vinnik, 1994], Rayleigh waves [Montagner and Tanimoto, 1991; Okal and Taylandier, 1980], and with P_n azimuthal anisotropy [Taylandier and Bouchon, 1979] in this region. Thus, we suggest that, in the southern Pacific, upper mantle anisotropy is primarily related to the process we modeled, i.e., a velocity gradient between the Pacific lithosphere and mesosphere.

The variability of SKS delay times may be ascribable to the activity of numerous hotspots in this area. Buoyant vertical flow should occur beneath an active hotspot and very little or no splitting would be detected by a vertically propagating wave in such a case (PPT). Localization of hotspot effects and a polarization direction parallel to the APM beneath older islands is consistent with a lithospheric thinning restricted to the region immediately beneath the plume conduit [Davies, 1994] and with an accumulation and drag (by the plate motion) of hot plume material in the asthenosphere [Sleep, 1994], leading to an enhanced asthenospheric deformation. Our models predict for a 80–100 My old fast plate ($v \geq 6 \text{ cm/y}$) delay times of 1.7–1.8 s. Discrepancy between measured and calculated delay times may be explained by partial destruction of the sub-horizontal upper mantle fabric due to hotspot activity, presence of partial melt in the asthenospheric layer, or the change in APM with time.

Fast-wave polarization directions are however closer to the fossil spreading direction at Hawaii (KIP, $\phi = 90^\circ$, $\delta t = 0.9$ s), indicating a departure from a simple, 2D upper mantle shearing due to the Pacific plate absolute motion relative to fixed deep mantle (hotspots reference frame). Our models suggest that ridge-related fabrics should only be preserved in a thin (~ 10 km), shallow mantle layer unless an abnormally rapid viscosity

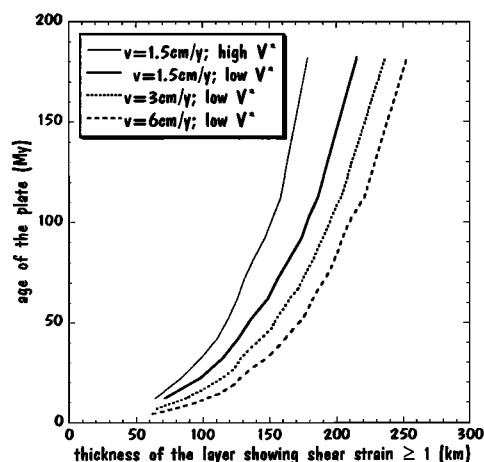


Figure 4. Dependence of the thickness of the layer displaying $\gamma \geq 1$ on dunitic activation volume V^* and age of the plate.

decrease occurs near the ridge. Lithosphere-asthenosphere boundary topography may yet affect asthenospheric flow [Bormann *et al.*, 1996]. KIP is situated on the Molokai fracture zone, which separates plate domains with different ages ($\Delta t \sim 10$ My) and may locally guide the asthenospheric flow.

Finally, SKS splitting measurements near oceanic ridges cannot be explained by a passive upper mantle flow beneath spreading plates. Ascension Island (ASC, $\phi = N83^\circ E$, $\delta t = 0.95$ s), Easter Island (RPN, $\phi = N14^\circ W$, $\delta t = 0.8$ s) and Iceland ($\phi = N20^\circ W$ - $N45^\circ W$, $\delta t = 0.7$ - 1.7 s [Bjarnason *et al.*, 1996]) are located on young (< 5 My old) seafloor. Our models show that even a fast plate cannot generate delay times higher than 0.5 s after only 5 My of displacement. We suggest that these measurements record the active, probably convection-related, flow of the upper mantle. The fast-wave polarization direction at Ascension is grossly parallel to both ridge spreading and APM, suggesting a divergent flow in the upper mantle parallel to the plate motion, but at a faster rate. At Easter Island and Iceland, the situation is more complicated: The fast-wave polarization direction measured is at a high angle to both spreading direction and APM. A departure of geometrically simple upper mantle flow patterns, like passive drag or radial flow away from a hotspot, must be invoked in the interpretation of this SKS splitting data.

Conclusions

The motion of an oceanic plate over a presumed stationary (slower or differently moving) mantle induces localized shearing in a thin (~ 100 km) layer at the base of the thermal lithosphere. As the plate cools, the upper part of the deformed layer freezes. For young plates, the thickness of the deformed layer initially increases rapidly with the age of the plate, due to plate cooling and deepening and widening of the shear zone, but this increase slows progressively. For plates of similar ages, the final thickness depends on the plate velocity.

Seismic anisotropy in an ocean basin will therefore result from both a frozen fabric in the lithosphere and a fabric generated by the present asthenospheric flow. These fabrics are parallel, forming a single anisotropic layer, unless absolute plate motion changes with time. In a plate moving with constant velocity, vertically propagating shear waves, as SKS, will have a fast wave polarized parallel to the plate motion direction. The delay time will depend on the thickness of the strained layer and on the intensity of crystallographic fabrics developed within this layer. If we assume that the whole layer displaying $\gamma \geq 1$ has a homogeneous anisotropy, the delay time will depend only on the thickness of the layer and on its intrinsic anisotropy. It will therefore increase away from the ridge at a progressively decreasing rate. For an intrinsic anisotropy of 4.25% in the vertical direction, we obtain delay times of 1.8-2.1 s for 180 My-old plates moving at 1.5 or 6 cm/y, respectively, from which ca. 20% is generated in the frozen lithospheric layer.

Analysis of seismic anisotropy data in oceanic basins suggests that, although this oversimplified model may provide a first approximation of mechanisms responsible for the development of seismic anisotropy in oceanic basins, the actual situation is far more complicated. Parallelism of fast wave polarization direction with the APM direction is common but not systematic. The large changes in plate motion observed in the Pacific may account for some of the discrepancy between measured and calculated values. However other processes, such as hotspot activity or departures from a large-scale 2D upper mantle flow (e.g., flow along fracture zones, small-scale convection), must be invoked to explain the lateral variation in delay times over relatively short distances in the southern Pacific, or the fast wave polarization

direction measured at KIP (Hawaii). Finally, SKS splitting measurements near oceanic ridges point to a significant contribution of active upper mantle flow to seismic anisotropy.

Acknowledgments. We thank E. Okal, C. Wolfe, and P. Silver for providing us their results prepublication. We thank L. Vinnik, A. Nicolas, F. Boudier and D. Mainprice for fruitful discussions, and D. Blackman, M. Savage, and an anonymous reviewer for their constructive reviews. R. Russo was supported by an NSF-NATO fellowship during this work. This paper is a contribution to NATO project # CRG950269.

References

- Bjarnason, I.T., C.J. Wolfe, S.C. Solomon, and G. Gudmundson, Initial results from the ICEMELT experiment: Body-wave delay times and shear wave splitting across Iceland, *Geophys. Res. Lett.*, **23**, 459-462, 1996.
- Bormann, P., G. Grunthal, R. Kind, and H. Montag, Upper mantle anisotropy underneath Central Europe: Effect of absolute motion and lithosphere-asthenosphere boundary topography?, *J. Geodyn.*, **22**, 11-32, 1996.
- Davies, G.F., Thermomechanical erosion of the lithosphere by mantle plumes, *J. Geophys. Res.*, **99**, 15,709-15,722, 1994.
- Farra, V., and L. Vinnik, Shear-wave splitting in the mantle of the Pacific, *Geophys. J. Int.*, **119**, 195-218, 1994.
- Froidevaux, C., and G. Schubert, Plate motion and structure of the continental asthenosphere: A realistic model for the upper mantle, *J. Geophys. Res.*, **80**, 2553-2564, 1975.
- Hirth, G., and D.L. Kohlstedt, Experimental constraints on the dynamics of the partially molten upper mantle: Deformation in the dislocation creep regime, *J. Geophys. Res.*, **100**, 15,441-15,449, 1995.
- Karato, S., and P. Wu, Rheology of the upper mantle: A synthesis, *Science*, **260**, 771-778, 1993.
- Mainprice, D., and P.G. Silver, Interpretation of SKS-waves using samples from the subcontinental lithosphere, *Phys. Earth Planet. Inter.*, **78**, 257-280, 1993.
- Meade, C., P. Silver, and S. Kaneshima, Laboratory and seismological observations of lower mantle anisotropy, *Geophys. Res. Lett.*, **22**, 11293-1296, 1995.
- Montagner, J.-P., and T. Tanimoto, Global upper mantle tomography of seismic velocities and anisotropy, *J. Geophys. Res.*, **96**, 20,337-20,351, 1991.
- Nicolas, A., and N.I. Christensen, Formation of anisotropy in upper mantle peridotites - A review, in *Composition, structure and dynamics of the lithosphere-asthenosphere system*, edited by K. Fuchs, and C. Froidevaux, pp. 111-123, AGU, Washington, D.C., 1987.
- Okal, E.A., and J. Taylandier, Rayleigh wave dispersion in french Polynesia, *Geophys. J. Royal Astron. Soc.*, **63**, 719-733, 1980.
- Schubert, G., C. Froidevaux, and D. Yuen, Oceanic lithosphere and asthenosphere: Thermal and mechanical structure, *J. Geophys. Res.*, **81**, 3525-3540, 1976.
- Silver, P.G., and W.W. Chan, Implications for continental structure and evolution from seismic anisotropy, *Nature*, **335**, 34-39, 1988.
- Silver, P.G., and W.W. Chan, Shear wave splitting and subcontinental mantle deformation, *J. Geophys. Res.*, **96**, 16429-16454, 1991.
- Sleep, N.H., Lithospheric thinning by midplate mantle plumes and the thermal history of hot plume material ponded at sublithospheric depths, *J. Geophys. Res.*, **99**, 9327-9343, 1994.
- Su, L., and J. Park, Anisotropy and the splitting of PS waves, *Phys. Earth Planet. Inter.*, **86**, 263-276, 1994.
- Taylandier, J., and M. Bouchon, Propagation of high-frequency Pn waves at great distances in the South Pacific and its implication for the structure of the lower lithosphere, *J. Geophys. Res.*, **88**, 5613-5619, 1979.
- Vinnik, L.P., V. Farra, and B. Romanovicz, Azimuthal anisotropy in the earth from observations of SKS at GEOSCOPE and NARS broadband stations, *Bull. Seismol. Soc. Am.*, **79**, 1542-1558, 1989.
- Vinnik, L.P., L.I. Makeyeva, A. Milev, and A.Y. Usenko, Global patterns of azimuthal anisotropy and deformations in the continental mantle, *Geophys. J. Int.*, **111**, 433-437, 1992.
- Zhang, S., and S. Karato, Lattice preferred orientation of olivine aggregates in simple shear, *Nature*, **375**, 774-777, 1995.

Raymond Russo, Andr ea Tommasi, and Alain Vauchez, Laboratoire de Tectonophysique, ISTEEM, USTL, F34095 Montpellier cedex 5, France; email: deia@dstu.univ-montp2.fr

(Received March 21, 1996; revised June 21, 1996; accepted August 13, 1996.)